Politecnico di Milano
Mathematical Engineering
Financial Engineering 2021/2022

Calibration and Monte Carlo for Additive Processes

Lepore Marco
Lunardi Chiara
Masatti Gabriele Giovanni

June 14, 2022

List of Figures

List of Tables

Contents

1 Introduction

Inspired by the works published in 2021 by our lecturers Baviera and Azzone we have had the opportunity, through the final project of the course of Financial Engineering, to deepen our knowledge about a well-known financial topic: Lévy Processes. In particular Lévy Normal Tempered Stable (LTS) processes have become a powerful modeling solution that provides parsimonious models consistent with option and underlying asset prices thanks to the fact that they do admit a simple closed formula (Carr and Madan 1999, Lewis 2001 (4)) to price the most liquid instruments (EU call options) allowing quite easy calibration and pricing (via Montecarlo simulations). However these models present a limit: they do not well reproduce market implied volatility smiles with sufficient precision as shown recently by financial literature. In order to overcome this problem a new, more advanced class of processes can be taken into account: Additive Tempered Stable (ATS) processes. The main difference is that ATS present independent, but time-inhomogeneous increments, differently from the ones of LTS processes (that enjoy time homogeneity). Our working path can be summarized as follows:

1. Calibration of the Forwards and Discount factors following the technique of synthetic forwards described in (3);
2. Calibration of an ATS NIG, using market data following (2), comparison of the precision with standard LTS NIG in reproducing volatility smiles and fitting of a power-law ATS process;
3. Simulation of an ATS NIG forward increment with Lewis-FFT algorithm and pricing of 30 European call options exploiting it, confronting the results with prices given by Lewis Formula & Quadrature rule;
4. Use of Lewis-FFT algorithm to simulate the underlying stock price of a Sprint Autocallable Put Option and pricing of this derivative instrument, followed by a comparison with classical Monte Carlo simulation of a LTS NIG process.

In the next section 2 we have briefly described the theoretical framework at the basis of our work, then we have proceeded with the presentation of the dataset used and the core of our project, respectively in 3 and 4 (where are presented the calibration, simulation and pricing). In the end, in section 5, we have concluded with the attempt of pricing an exotic derivative as previously described.

2 Modeling Framework

As introduced in 1 the main goals of our work have been:

- ★ The calibration at different dates of σ_t, k_t and η_t, that characterize Additive Tempered Stable processes, a generalization of Lévy Normal Tempered Stable processes involving time-dependent parameters;
- ★ The simulation of ATS processes exploiting a Monte Carlo technique, based on the numerical inversion of the cumulative distribution function of process increments, in order to price plain vanilla European call options;
- ★ The pricing of a Sprint Autocallable Put Option (an exotic path-dependent derivative) with the underlying stock price simulated as above.

In the following subsections we have briefly summarized the key theoretical concepts at the basis of the techniques used for our purposes.

2.1. LTS

Lévy Normal Tempered Stable processes (LTS) are commonly used in the financial industry for derivative pricing, being rather flexible and involving very few parameters. According to this modeling approach, the price of a forward contract with expiry T at a time instant $t < T$ is described via an exponential Lévy process, i.e.:

$$F_t(T) = F_0(T)e^{f_t}$$

with f_t a LTS

$$f_t = -\left(\frac{1}{2} + \eta\right)\sigma^2 S_t + \sigma W_{S_t} + \phi t$$

where η, σ are two real parameters $\eta \in \mathbb{R}$, $\sigma \in \mathbb{R}^+$, while ϕ is obtained by imposing the martingale condition on $F_t(T)$. W_t is a Brownian motion and S_t is a Lévy Tempered Stable Subordinator independent from the Brownian motion with variance per unit of time k. Examples of LTS subordinators are the Inverse Gaussian process for NIG (the one we focused on in this project) and the Gamma process for the VG. It is possible to write the characteristic function of f_t as:

$$E\left[e^{iuf_t}\right] = \mathcal{L}_t\left(iu\left(\frac{1}{2} + \eta\right)\sigma^2 + \frac{u^2\sigma^2}{2}; k, \alpha\right)e^{iu\varphi t}$$

where $\alpha \in [0, 1)$ is the LTS index of stability and $\mathcal{L}_t$ is the Laplace transform of S_t:

$$\ln \mathcal{L}_t\left(u; k; \alpha\right) = \begin{cases} \frac{t}{k}\frac{1-\alpha}{\alpha}\left\{1 - \left(1 + \frac{uk}{1-\alpha}\right)^2\right\} & if\ \ 0 < \alpha < 1 \\ -\frac{t}{k}\ln\left(1 + uk\right) & if\ \ \alpha = 0 \end{cases}$$

The parameters that characterize these processes are: σ, which controls the average level of the volatility surface; k, which is related to the convexity of the implied volatility surface

and η which is linked to the volatility skew. Unfortunately, in this modeling approach the parameters' values are constant in time and it has been shown that LTS processes do not properly describe the implied volatilities that are observed in market data at different time horizons. For these reasons we have taken into account the following extension of LTS.

2.2. ATS

Additive Tempered Stable processes are a generalization of LTS processes that maintain the increments' independence, but allow for time-inhomogeneous parameters. They are described by a characteristic function of the same type of 2.1. but with time-dependent parameters:

$$E\left[e^{iuf_t}\right] = \mathcal{L}_t\left(iu\left(\frac{1}{2}+\eta_t\right)\sigma_t^2 + \frac{u^2\sigma_t^2}{2}; k_t, \alpha\right)e^{iu\varphi_t t}$$

where σ_t, k_t are continuous on $[0, \infty)$ and η_t, ϕ_t are continuous on $(0, \infty)$ with $\sigma_t > 0$, $k_t \geq 0$, $\phi_t t$ goes to zero as t goes to zero, $\alpha \in [0, 1)$ and as in the LTS case the forward price $F_t(T)$ is considered as the exponential of this ATS process $\{f_t\}_{t\geq 0}$. The deterministic function of time ϕ_t can be chosen s.t. the process $F_t(T)$ satisfies the martingality condition:

$$\phi_t(-i) = 1$$

From which it can be deduced:

$$\phi_t t = -\ln \mathcal{L}_t(\sigma_t^2\eta_t; k_t, \alpha)$$

The following Theorem states some conditions that must be verified in order to ensure the existence of an ATS process.

Theorem 1 Sufficient conditions for the existence of ATS
There exists an additive process $\{f_t\}_{t\geq 0}$ with the characteristic function 2.2. if the following two conditions hold.

1. *$g_1(t)$, $g_2(t)$ and $g_3(t)$ are non decreasing, where*

   $g_1(t) := (1/2+\eta_t) - \sqrt{(1/2+\eta_t)^2 + 2(1-\alpha)/(\sigma_t^2 k_t)}$

   $g_2(t) := -(1/2+\eta_t) - \sqrt{(1/2+\eta_t)^2 + 2(1-\alpha)/(\sigma_t^2 k_t)}$

   $g_3(t) := \frac{t^{1/\alpha}\sigma_t^2}{k_t^{(1-\alpha)/\alpha}}\sqrt{(1/2+\eta_t)^2 + 2(1-\alpha)/(\sigma_t^2 k_t)};$

2. *Both $t\sigma_t^2\eta_t$ and $t\sigma_t^{2\alpha}\eta_t^{\alpha}/k_t^{1-\alpha}$ go to zero as t goes to zero.*

The main advantage of this class of models is the possibility to fit in a very precise way the volatility term structure, maintaining the parsimony of LTS processes.
In this modeling approach the calibrated parameters σ_t, η_t, k_t are vectors, where each element is related to a specific expiry.

2.3. Power-law scaling ATS

The Power-law scaling ATS is a subcase of ATS characterized by self-similar functions of time. This model description is particularly accurate in describing the market-implied volatility surfaces. Furthermore, through Power-law scaling functions of time it is possible to rewrite Theorem 1 conditions as inequalities on the scaling parameters, as stated in the following Theorem.

Theorem 2 Power-law scaling ATS
There exists an ATS with

$$k_t = \bar{k}\, t^{\beta} \qquad \eta_t = \bar{\eta}\, t^{\delta} \qquad \sigma_t = \bar{\sigma}$$

where $\alpha \in [0, 1)$, $\bar{\sigma}, \bar{k}, \bar{\eta} \in \mathbb{R}^+$ *and* $\beta, \delta \in \mathbb{R}$ *that satisfy the following conditions:*

1. $0 \leq \beta \leq \frac{1}{1-\alpha/2}$;
2. $-\min(\beta, \frac{1-\beta(1-\alpha)}{\alpha}) < \delta \leq 0$;

where the second condition reduces to $-\beta < \delta \leq 0$ *for* $\alpha = 0$.
In our work we have fitted a Power-law ATS in order to estimate the scaling parameters.

2.4. Monte Carlo simulation for additive processes

Additive normal tempered stable processes are used in order to simulate the underlying of derivatives (also path dependent ones) for pricing purposes.
This requires simulations of ATS increments. However in general for most additive processes, the law of increments is not explicitly known.
To overcome this problem, as described in (1), we have exploited a MC technique for additive processes based on a numerical inversion of the cumulative distribution function, obtained shifting the integration path within the characteristic function horizontal analyticity strip. As stressed before the characteristic function $\Phi_t(u) = E\left[e^{iuf_t}\right]$ of an additive process f_t admits a closed formula. Moreover according to Lukacs Theorem, this $\Phi_t(u)$ is analytic in a horizontal strip delimited on the imaginary axis by $(-(p_t^+ + 1), p_t^-)$.
In case of Lévy processes, the increment $f_t - f_s$ has the same distribution as f_Δ, where $\Delta = t - s$, however, due to time inhomogeneity, this property can not be generalized to additive processes. For an additive process, thanks to independent increment property, the characteristic function of an increment is:

$$\Phi_{s,t}(u) = E\left[e^{iu(f_t - f_s)}\right] = \frac{E\left[e^{iuf_t}\right]}{E\left[e^{iuf_s}\right]}$$

It is possible to use the Monte Carlo method for ATS if some assumptions hold:

Assumption 1 p_t^+ and p_t^- are non increasing in t.

Under this first assumption it is possible to obtain the CDF from the characteristic function of the increment shifting of -ia (with a real constant such that a $\in (-p_t^-, p_t^+ + 1)$) the integration path within the characteristic function horizontal analyticity strip.
We have focused on $a > 0$ being this a default choice in the equity case. The CDF of an additive process increment is:

$$P(x) = 1 - \frac{e^{-ax}}{\pi} \int_0^{+\infty} du Re\left[\frac{e^{-iux}\phi_{s,t}(u - ia)}{iu + a}\right]$$

And an approximation through a discrete Fourier transform is:

$$\hat{P}(x) = 1 - \frac{e^{-ax}}{\pi} \sum_{l=0}^{N-1} Re\left[\frac{e^{-i(l+1/2)hx}\phi_{s,t}((l + 1/2)h - ia)}{i(l + 1/2)h + a}\right] h$$

where h is the step size in the Fourier domain and N is the number of points in the grid.

Assumption 2 $\forall\, t > s \geq 0$ there exists $B > 0$, $b > 0$ and $\omega > 0$ such that, for sufficiently large u, the following bound for the absolute value of the characteristic function holds:

$$|\Phi_{s,t}(u - ia)| < Be^{-bu^{\omega}} \qquad \forall a \in (0, p_t^+ + 1)$$

The computation of the CDF is subject to two sources of error: a discretization error, due to the fact that the integrand is evaluated only at the grid points, and a range error, because of the approximation with a finite sum. Nevertheless under Assumptions 1 and 2 it is possible to bound numerical errors for the CDF, and to select the optimal integration path that minimizes this error bound, choosing the shift a $= (p_t^+ + 1)/2$, as stated in Proposition 2.1 of (1).
After having computed an approximation $\hat{P}$ of the CDF, exploiting the Fast Fourier Transform algorithm, the simulation method consists in inverting the $\hat{P}$ such that it is possible to sample the process X (performing an interpolation) as $X = \hat{P}^{-1}(U)$, where U is a sampling vector of a uniform random variable in [0, 1].

3 Dataset

The dataset we have used is composed of real market quotes (no smoothing or interpolation), containing calls and puts of SP 500 index for every liquid maturity. It is worth noticing that the options on this index are some of the most liquid ones in the equity market at a world level.
The dataset contains all bid/ask, opening and high prices for both calls and puts. The strikes were in ascending order in a regular grid for each available maturity. We have excluded options that did not satisfy two simple liquidity constraints:

i. We have discarded options whose (mid-market) price was less than 10% the minimum difference in the grid of market strikes (the so-called "penny options");

ii. We have discarded options with bid-ask spread over bid price bigger than 60%.

After imposing these two conditions above we have obtained a new dataset where, for some strikes, either a call or a put was missing. Since we needed both for each strike we have decided to discard these cases.
We obtained a dataset composed of 1388 options, calls and puts in the same quantity. We have reported in this table the number of calls and puts for every maturity:

Options Number	Calls Number	Puts Number	Maturity
22	11	11	'21-Jun-2019'
48	24	24	'19-Jul-2019'
70	35	35	'16-Aug-2019'
92	46	46	'20-Sep-2019'
106	53	53	'18-Oct-2019'
112	56	56	'15-Nov-2019'
128	64	64	'20-Dec-2019'
134	67	67	'17-Jan-2020'
148	74	74	'20-Mar-2020'
166	83	83	'19-Jun-2020'
180	90	90	'18-Dec-2020'
182	91	91	'17-Dec-2021'

Table 1: Dataset Options S&P 500

4 Project

4.1. Calibration of Forwards and Discount Factors

We have calibrated the Forward and Discount Factors following the technique described in (3). This approach allows to obtain the implicit interest rates using only option prices and a no-arbitrage condition on an option portfolio known as synthetic forward. In our clean dataset bid and ask prices of calls and puts were provided for different strikes at each liquid maturity. Thanks to the absence of arbitrage condition the put-call parity at value date t_0 and maturity T for European options, with respect to the forward price F and the strike price K, is:

$$C(K) - P(K) = \overline{B}(t_0, T)(F - K)$$

Where $\overline{B}(t_0, T)$ is the market discount factor. A synthetic forward G(K) with maturity T is a portfolio that comprises of a long call and a short put at a given strike price K. So the previous equation becomes:

$$F = \frac{G(K)}{\overline{B}(t_0, T)} + K$$

By non-arbitrage principle, forward prices F in t_0 with the same maturity T should be constant whatever strike K. So the market implied discount factor is the unique factor such that the forward price does not depend on K; thus this is a linear problem in F and $\overline{B}$.
The bid synthetic forward is obtained by selling the call and buying the corresponding put, vice-versa for the ask price. Mid prices are the arithmetic average of bid and ask prices.

$$\begin{cases} G^{bid}(K) = C^{bid}(K) - P^{ask}(K) \\ G^{ask}(K) = C^{ask}(K) - P^{bid}(K) \\ G(K) = \dfrac{G^{bid}(K) + G^{ask}(K)}{2} \end{cases}$$

In order to calibrate the Forward and the Discount Factors for every maturity we have performed the following linear regression:

$$G_i = -\overline{B}(t_0, T) K_i + \overline{B}(t_0, T) F + \varepsilon_i$$

for the different strikes K_i i=1,..,N available at value date t_0 and maturity T, where ϵ_i are some error variables. From this procedure $\overline{B}(t_0, T)$ is obtained as the angular coefficient and the Forwards as the intercept divided by the Discount Factor.
The explicit formula of the least squares estimation is:

$$\overline{B}(t_0, T) = -\frac{\sum_{i=1}^{N} \left(Ki - \widehat{K}\right)\left(G_i - \widehat{G}\right)}{\sum_{i=1}^{N} \left(Ki - \widehat{K}\right)^2}$$

Where

$$\widehat{G} = \frac{1}{N} \sum_{i=1}^{N} Gi$$

$$\widehat{K} = \frac{1}{N} \sum_{i=1}^{N} Ki$$

In figures (1) and (2) we can observe respectively the bootstrapped discounts, and the forwards with their confidence intervals, in function of the different maturities.

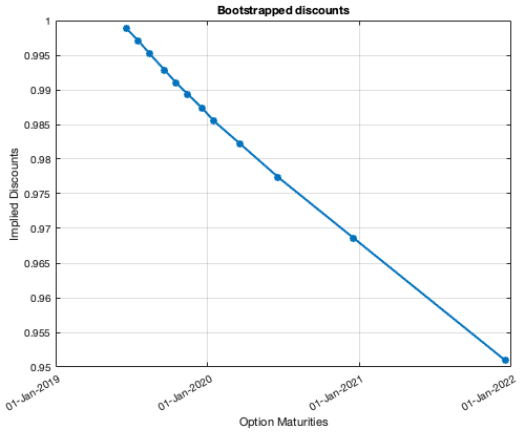

Figure 1: Calibrated Discount Factors

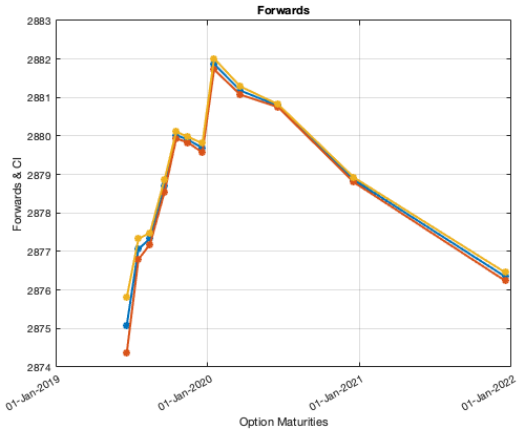

Figure 2: Calibrated Forwards

$\overline{B}(t_0, T)$	F	Maturity
0.9988	2875.08	'21-Jun-2019'
0.9971	2877.06	'19-Jul-2019'
0.9952	2877.34	'16-Aug-2019'
0.9929	2878.71	'20-Sep-2019'
0.9910	2880.03	'18-Oct-2019'
0.9894	2879.90	'15-Nov-2019'
0.9873	2879.69	'20-Dec-2019'
0.9855	2881.87	'17-Jan-2020'
0.9822	2881.18	'20-Mar-2020'
0.9774	2880.78	'19-Jun-2020'
0.9686	2878.86	'18-Dec-2020'
0.9510	2876.35	'17-Dec-2021'

Table 2: Bootstrapped discounts & Forward prices

The regression results are very precise having an R^2 above 0.999995 for all maturities T in the dataset analyzed.

4.2. Calibration of ATS NIG process

As described in 2.2. ATS NIG process presents 3 time-dependent parameters: σ_t, k_t and η_t. Thus for the calibration of the model, following the technique described in (2) we have "cut" the volatility surface into slices, each one containing options with the same maturity, and we have proceeded slice by slice. Indeed for every fixed T it is possible to define a different LTS NIG model such that, at that T, its marginal distribution is equal to the marginal distribution of the corresponding ATS. In the following all the steps are commented into detail:

4.2.1 Choice of options

To calibrate our model we have taken into account only options of S&P 500 that satisfied the conditions in 3 with the following twelve maturities: 21-Jun-2019, 19-Jul-2019, 16-Aug-2019, 20-Sep-2019, 18-Oct-2019, 15-Nov-2019, 20-Dec-2019, 17-Jan-2020, 20-Mar-2020, 19-Jun-2020, 18-Dec-2020, 17-Dec-2021, thus obtaining three vectors of parameters of twelve components. We have considered both call and put options, but used just the out of the money ones. For the sake of completeness we have tried also to calibrate on in the money options obtaining similar results, but in the end we have preferred to rely upon OTM options since they're more liquid in the markets and in general present prices with smaller bid-ask spreads. We have reported the results of the calibration on ITM options in the Appendix A.

4.2.2 Minimization & Constraints

Having the set of initial Forward prices for each maturity and the corresponding discount factors, we have minimized the sum of the squared distances between the prices given by the closed Lewis formula and the market ones; for call options we have applied directly Lewis formula, while for the puts we have exploited put-call parity as below:

$$\frac{C(x)}{B(t_0,t)F_0} = 1 - e^{-\frac{x}{2}} \int_{-\infty}^{+\infty} \frac{d\xi}{2\pi} e^{-iz\xi} \phi(-\xi - \frac{i}{2}) \frac{1}{\xi^2 + 1/4}$$

$$C(t_0,T) - P(t_0,T) = B(t_0,T)(F(t_0,T) - K)$$

Where $x = \ln(\frac{F0}{K})$ is the moneyness. We have proceeded in this way maturity by maturity using `fmincon` as minimizer, thanks to which we have been able to impose the monotonicity constraints of Theorem 1 2.2. and the one of NIG. In the first step we have imposed only the analiticity strip condition:

$$\eta < -\underline{\omega}$$

with $\underline{\omega} = \frac{1-\alpha}{\eta_t \sigma_t^2}$. While, besides the former, at each following time step we computed $g_1(t-1)$, $g_2(t-1)$ and $g_3(t-1)$ with σ_{t-1}, η_{t-1} and k_{t-1} coming from the previous step and $g_1(t)$, $g_2(t)$ and $g_3(t)$ as function handles of σ_t, η_t and k_t. Then we passed as a constraint to `fmincon` $g_1(t-1) \leq g_1(t)$, $g_2(t-1) \leq g_2(t)$ and $g_3(t-1) \leq g_3(t)$ together with the analiticity condition. Another possibility could be to use another faster minimizer implementing a penalty algorithm, but we have preferred to rely on `fmincon` to be sure of the precision

of the results. The plots of g1, g2 and g3, computed with parameters obtained with the calibration at each time step are reported below. As it is visible they are non-decreasing with respect to time.

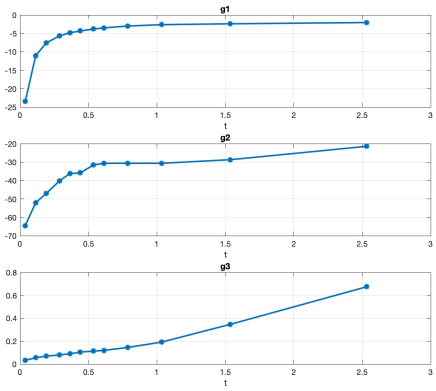

Figure 3: g1, g2 & g3

4.2.3 Smiles reproduction & performances

For every different maturity we have then confronted the implied volatility smile of ATS and the one of the market data, obtaining very good results. The precision is particularly visible for shorter maturities. Below are reported the results for the first, an intermediate and the last maturity. Plots are made with respect to the moneyness, considered as $\log(\frac{K}{F0})$ and also the MSE of prices are reported. As it can be seen these latter are really small. In order to have a benchmark to confront our results we have calibrated also an LTS NIG on the whole volatility surface obtaining good results, but a precision well below the one of the ATS. In figures (5), (7) and (9) are reported the reproduction of the same smiles obtained using LTS NIG. MSE errors computed on prices are on average two orders of magnitude greater than the ones of ATS NIG and the greater accuracy is more marked for short maturities (figures (4), (5)).

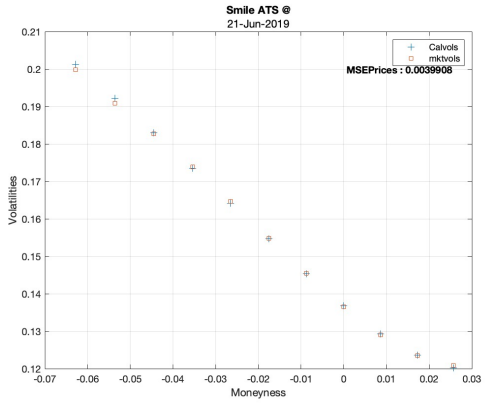

Figure 4: First maturity smile

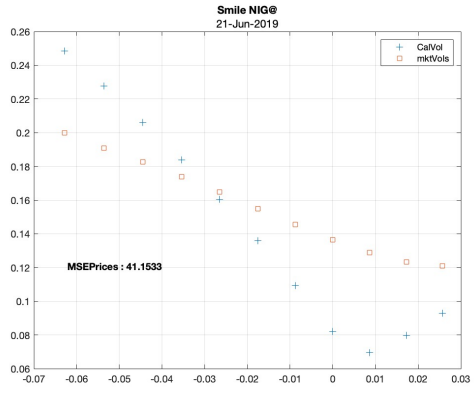

Figure 5: First maturity smile NIG

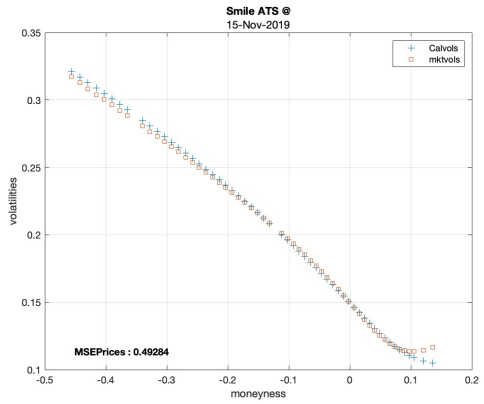

Figure 6: Intermediate maturity smile ATS

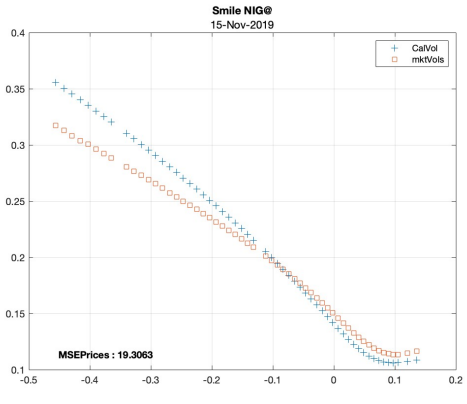

Figure 7: Intermediate maturity smile NIG

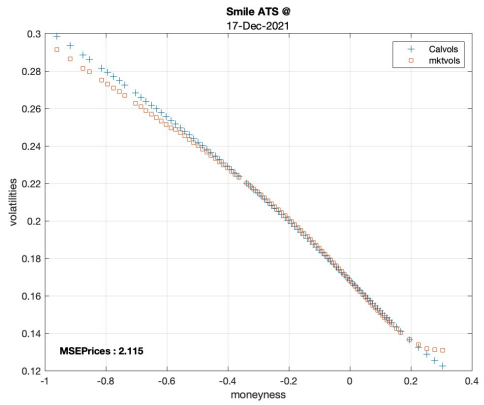

Figure 8: Last maturity smile ATS

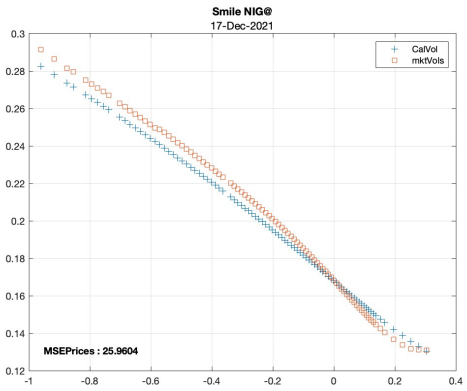

Figure 9: Last maturity smile NIG

To have a further comparison we have also plotted the behavior of the mean squared error to which we have applied the log10 scaling in order to better show the improvement using ATS.

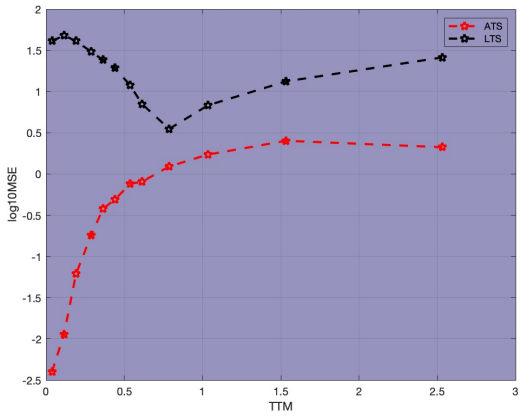

Figure 10: Error comparison

Furthermore we have confronted the market volatility skew, which we have considered as the difference between the last and the first option implied volatilities, with the one reproduced by our model, obtaining the results shown by the graph below.

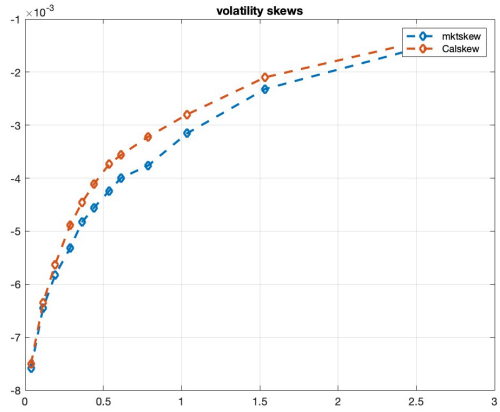

Figure 11: Error comparison

It is possible to notice that skews are all really small since we have considered in the calibration only OTM options, having small variations in implied volatilities. ATS NIG performs almost perfectly for the first maturities, while there are some very small discrepancies for later ones. Indeed sometimes the calibration was slightly less accurate on very OTM options, thus providing us with dissimilar differences between last and first implied volatilities. We have tried to fix this problem imposing some weights on the calibration (as the inverse of the vega of the options to power two), but then we turned with the opposite problem. Since our results seemed to be enough satisfying we have decided not to impose any weight on the calibration, having the less OTM options perfectly calibrated for each maturity.
In the end the table below displays MSE and MAPE of ATS NIG and LTS NIG for the three maturities chosen.

Maturity	LTS MAPE	ATS MAPE	LTS MSE	ATS MSE
21-Jun-2019	55.9951 %	0.9938 %	41.1533	0.004
15-Nov-2019	32.2629 %	5.1721 %	19.3063	0.4928
17-Dec-2021	7.6313 %	3.6061 %	25.9603	2.1150

Table 3: Calibration performances

It immediately jumps to the eye how relevant is the improvement of ATS NIG especially for short maturities where classical LTS NIG is very inaccurate.

4.3. Power-law ATS fitting

In this section we have reported the fit of a Power-law ATS to estimate the scaling parameters. Then we have checked if the obtained parameters are coherent with the calibrated ones and satisfy the conditions for the existence of an ATS process.
As described by R. Baviera and M. Azzone in (2) and stated in 2.3., the power-law scaling ATS is characterized by parameters with the following behaviour:

$$k_t = \bar{k}\, t^{\beta} \qquad \eta_t = \bar{\eta}\, t^{\delta} \qquad \sigma_t = \bar{\sigma}$$

In order to estimate the scaling parameters of this model it is possible to rewrite the problem in log-log scale as:

$$\begin{cases} ln(\hat{k}_t) := ln(\bar{k}) + \beta ln(t) \\ ln(\hat{\eta}_t) := ln(\bar{\eta}) + \delta ln(t) \end{cases}$$

Proceeding in this way we have then implemented linear regressions over $ln(\hat{k}_t)$, $ln(\hat{\eta}_t)$, deriving from them the coefficients β and δ and the intercepts $ln(\bar{k})$ and $ln(\bar{\eta})$ of the regression lines.
The estimated values are:

β	δ	$\bar{k}$	$\bar{\eta}$	$\bar{\sigma}$
0.99	-0.26	0.97	12.41	0.11

Table 4: Fitted parameters

Particularly focusing on the regressions over $ln(\hat{k}_t)$ and $ln(\hat{\eta}_t)$ in both the cases we have obtained good results, indeed the R^2 of the model are very high over 0.95 for both, and the p-values of the models are of the order of 10^{-9} in the former case and 10^{-8} in the latter, ensuring the statistical significance of the models. Moreover we have plotted below the regression lines obtained in these two cases:

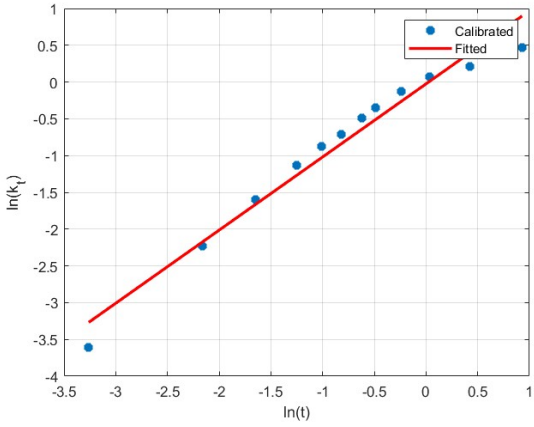

Figure 12: Regression line: $ln(\hat{k}_t) := ln(\bar{k}) + \beta ln(t)$

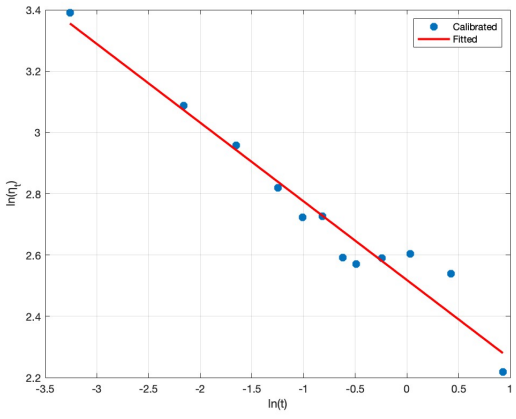

Figure 13: Regression line: $ln(\hat{\eta}_t) := ln(\bar{\eta}) + \delta ln(t)$

After the estimation of the parameters β and δ, we have checked the conditions of Theorem 2 on the scaling parameters, obtaining positive results for both.

$$\begin{cases} 0 \leq \beta \leq \frac{1}{1-\alpha/2} \\ \\ - \min(\beta, \frac{1-\beta(1-\alpha)}{\alpha}) < \delta \leq 0 \end{cases}$$

4.4. ATS forward increment simulation

Following the work of Baviera & Azzone in (1) we have implemented in matlab a function to simulate a forward increment of an ATS NIG process with a Monte Carlo simulation technique called Lewis FFT algorithm.

4.4.1 Assumptions

First of all we had to verify if Assumptions 1 and 2 in 2.4. were satisfied, so we have selected b, B and ω very close to the right (1 bp) end point of the following bounds, suggested by (1):

$$log(B) > \frac{1-\alpha}{\alpha}\left(\frac{t}{k_t} - \frac{s}{k_s}\right), \qquad 0 < b < \frac{(1-\alpha)^{1-\alpha}}{2^\alpha \alpha}\left(\frac{t}{k_t^{1-\alpha}}\sigma_t^{2\alpha} - \frac{s}{k_s^{1-\alpha}}\sigma_s^{2\alpha}\right), \qquad 0 < \omega < 2\alpha$$

For these values we have observed that both p_t^+ and p_t^- were non-increasing and that $|\phi_{s,t}(u - ia)| < Be^{-bu^\omega}$ for sufficiently large values of u as shown by these two figures:

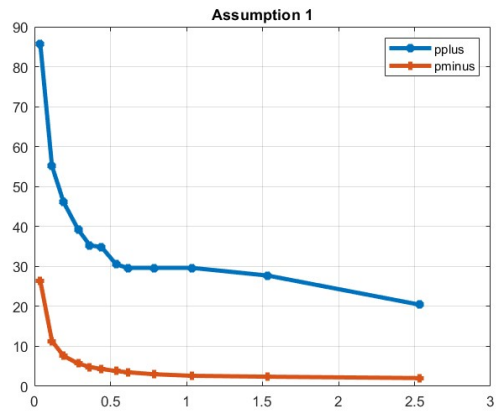

Figure 14: Assumption 1 verified

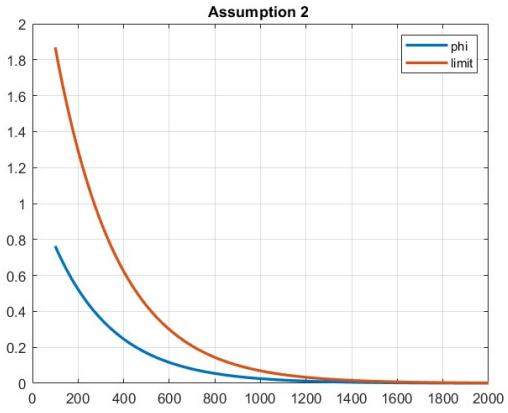

Figure 15: Assumption 2 verified, t = 17-Jan-2020, s = 20-Dec-2019

Moreover in order to have the smallest possible numerical error we have chosen $a = \frac{p_t^+ + 1}{2}$ where $p_t^+ = -g_2(t) - 1$.

4.4.2 Computation of the CDF

Then we have computed the numerical approximation of the CDF of the process forward increment 2.4. through Fast Fourier Transform algorithm. We have selected symmetric regular grids to discretize x and u (respectively the variable of the CDF and the variable of integration of the Fourier transform), going respectively from x_0 to x_k and from z_1 to z_n with step sizes γ and h. The latter have been computed through the following relations:

$$h(N) = \left(\frac{\pi(p_t^+ + 1)}{bN^\omega}\right)^{\frac{1}{\omega+1}}$$

$$\gamma = \frac{2\pi}{Nh}$$

Where $N = 2^M$ is the number of points in the grids with M an integer number. FFT algorithm provide us with very fast computational times evaluating directly the CDF on the whole x-grid passed as input; for completeness we have tried also to repeat the algorithm using the summation in 2.4. and evaluating the resulting function handle in every point of the grid, using `arrayfun`. As expected the computational time of FFT has revealed to be hugely inferior: 0.121792 seconds for FFT vs 5.195423 seconds for the sum.

4.4.3 Adjustments

After having computed an approximation $\hat{P}$ of the CDF, the algorithm required us to perform an inversion of it setting $X = \hat{P}^{-1}(U)$. So we had to ensure an increasing behaviour of $\hat{P}$ inside the interval [0, 1]. For this reason we have truncated the previous grid to an equally spaced sub-grid (with step γ) between two values $x_0 < 0$ and $x_k > 0$ ($K \leq N$). The choice of x_0 and x_k is driven by the minimization of the truncation error in the following way: we have selected a symmetric interval, with x_0 the nearest point to $-D\sqrt{t-s}$ on the grid in which the CDF has been computed. While we have kept the previous grid in the cases when $-D\sqrt{t-s}$ was outside our initial domain. We have chosen $D = 5$ as suggested in (1). Since even in this resized grid, for some time intervals, the CDF presented some numerical instabilities (oscillations for great negative values of x) we have decided to consider the region where it was strictly increasing and positive, putting to zero the remaining value, as described in (1). Thanks to these adjustments we have obtained a well-behaving, monotonic function for each possible forward time increment. Below we have reported a plot of the CDF obtained and of the corresponding PDF for a time increment of approximately one month:

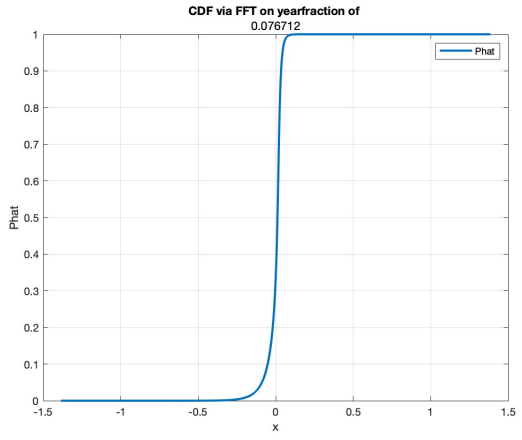

Figure 16: CDF between s = 21-jun-2019, t = 19-Jul-2019

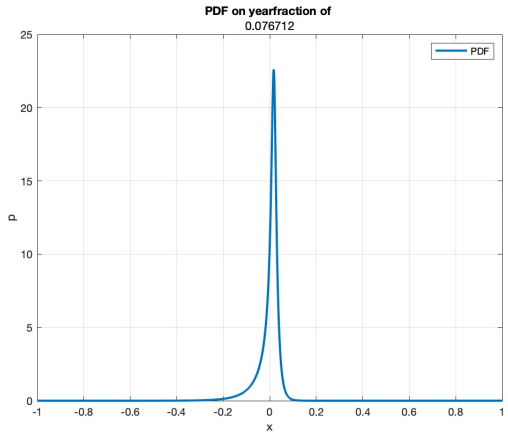

Figure 17: PDF between s = 21-jun-2019, t = 19-Jul-2019

4.4.4 Simulation of a forward increment

The numerical inversion to get the simulated process X has been performed through interpolation, indeed we first have generated 10^6 samples of a uniformly distributed random variable with values in [0, 1], and then we have used the matlab function `interp1` to interpolate the values:

$$X = \texttt{interp1}(\hat{P}(x), x, U)$$

With x the elements of the chosen grid. We have tried both with spline and linear interpolation: in the former case (as we have analyzed in the next section 4.5.) the interpolation error is significantly lower, with a small increase in the computational cost. However we have noticed that in some cases `interp1` with spline technique failed, especially for values between 0 and the first non null value of the CDF. When this happened we have used Akima interpolation in these points. Another possibility could be to simulate U between the minimum and the maximum of our CDF values as suggested by (5). Nevertheless in this latter case a lot of randomization is lost and thus the result differs too much from the linear case in our opinion. Because of that we have decided to proceed according to the former approach.

4.4.5 Simulation of underlying price S

Once able to simulate a forward ATS increment $f_t - f_s$ with $t > s > 0$ the simulation of the underlying price S directly follows from Garman-Kohlhagen relation (reported below) between forward prices and stock underlying prices and the fact that at the maturity of the forward, its price do coincide with the one of the underlying.

$$F(t_0, t) = S_0 e^{(r_t - d_t)(t - t_0)}$$

Having simulated $f_t - f_s$ as before, it is sufficient to obtain F(s, t) using the relation above, where the initial value of S_s can be computed as:

$$S_s = F(t_0, s) e^{f_s - f_0}$$

using the simulation of a forward increment with initial point 0. In the end:

$$S_t = F(s, t) e^{f_t - f_s}$$

It is worth noticing that S_t can be also directly simulated as below, but this would not exploit the simulation of a forward increment of the ATS process:

$$S_t = F(t_0, t) e^{f_t - f_0}$$

For completeness we have compared the two results in our code checking that they were equivalent.

4.5. European call options pricing

Exploiting the simulation of the ATS NIG forward increment, through the Lewis-FFT algorithm, we have priced 30 European call options with log-moneyness in a regular grid with range $\sqrt{t}(-0.2, 0.2)$ and maturity the 19^{th} of June 2019. The parameters σ_t, k_t and η_t used are the ones that characterize a power-law scaling ATS process, so we took into account the β, δ, $\bar{k}$, $\bar{\eta}$ and $\bar{\sigma}$ estimated previously when fitting a power-law , so we have considered the values from the table in 4.3.. We have also priced the options using the closed Lewis formula and then compared the results with the prices obtained via simulation method. In the latter approach we computed the prices using the Lewis formula:

$$\mathcal{C}(\mathcal{K}, \mathcal{T}) = B(t_0, T)F_0(T)\left\{1 - e^{-x/2}\int_{-\infty}^{+\infty}\frac{dz}{2\pi}e^{-izx}\phi^c(-z - \frac{i}{2})\frac{1}{z^2+\frac{1}{4}}\right\}$$

Where $\phi^c(u)$ is the characteristic function of f_T and x is the moneyness $x := ln\frac{F_0(T)}{K}$. The characteristic function is given by:

$$\phi^c(u) = e^{-iuln\mathcal{L}[\eta_t]}\mathcal{L}\left(\frac{u^2\sigma_t^2}{2} + iu(\frac{1}{2} + \eta_t)\sigma_t^2\right)$$

And the Laplace exponent function is:

$$ln\mathcal{L}[\omega] = \frac{t}{k_t}\frac{1-\alpha}{\alpha}\left[1 - \left(1 + \frac{k_t\omega\sigma_t^2}{1-\alpha}\right)^{\alpha}\right]$$

We have computed the integral both with the Quadrature method, exploiting the adaptive Gauss-Kronrod quadrature already implemented in Matlab by the function `quadgk`, and through the Fast Fourier Transform approach: $\hat{f}(z) \sim dx\sum_{j=1}^{N} f(x_j)e^{-ix_jz_k}$. In order to use the FFT method we have chosen the most suitable parameters $(M, x_1, N, dx, dz, z_1, x_N, z_N)$ with the optimization algorithm `lsqnonlin`. The pricing approach with the Lewis-FFT-S method is based on the simulation of the ATS forward increment obtained with the procedure explained in subsection 4.4., where the ATS process is obtained inverting the CDF performing the spline interpolation. Indeed we have simulated the process f_T taking into account 10^6 simulations, then according to Additive Normal Tempered Stable processes model:

$$F_T = F_0e^{f_T}$$

And then we got the prices of the call options as the discounted mean of the simulated payoffs:

$$C(x, T) = B(0, T)\frac{1}{N}\sum_{i=1}^{N} max\{F_T^i - K, 0\}$$

Moreover we have also computed the confidence intervals of the prices at 95% level. In the end we have evaluated the performance of Lewis-FFT-S and Lewis-FFT-L algorithms through three different measures of the error:

1. Root Mean Square-Error: $RMSE = \sqrt{\frac{1}{30}\sum_{i=1}^{30}(C^i_{LewisFormula} - C^i_{Lewis-FFT-S})^2}$;
2. Mean Absolute Percentage Error: $MAPE = \frac{1}{30}\sum_{i=1}^{30}\frac{|C^i_{LewisFormula} - C^i_{Lewis-FFT-S}|}{C^i_{LewisFormula}}100$;
3. Maximum Error: $MAXERR = max\{|C^i_{LewisFormula} - C^i_{Lewis-FFT-S}|\}$;

The results obtained in the lower and higher moneyness cases, taking into account M = 12 and 10^6 simulations are:

	$C_{LewisFormula}$	$C_{Lewis-FFT-S}$	$C_{Lewis-FFT-L}$
$x = -0.2\sqrt{t}$	0.6696 €	0.6721 €	0.6726 €
$x = 0.2\sqrt{t}$	106.7994 €	106.8830 €	106.8837 €

Table 5: Call prices

	RMSE	MAPE	MAXERR
Spline	0.0481	0.1819%	0.0836
Linear	0.0498	0.2112%	0.0843

Table 6: Call errors

Prices obtained with the three methods are reported below:

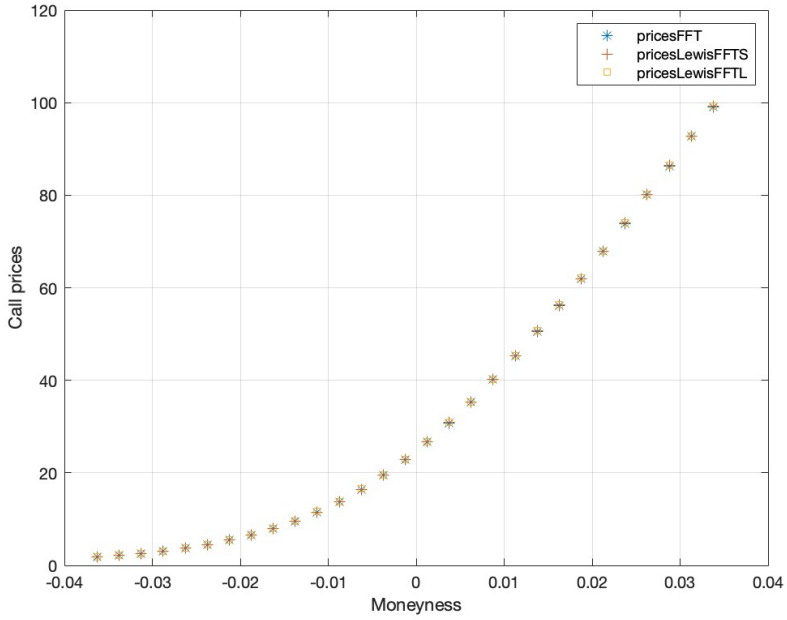

Figure 18: Call prices varying the moneyness

Comparing the results obtained via closed Lewis formula, Lewis-FFT algorithm with spline interpolation and Lewis-FFT algorithm with linear interpolation, as expected the measures of error are higher in this latter procedure.

We have plotted the obtained results varying $M \in [7, 13]$ and considering the $\log_{10} MAXERR$ in all the cases for both the Spline and Linear case.

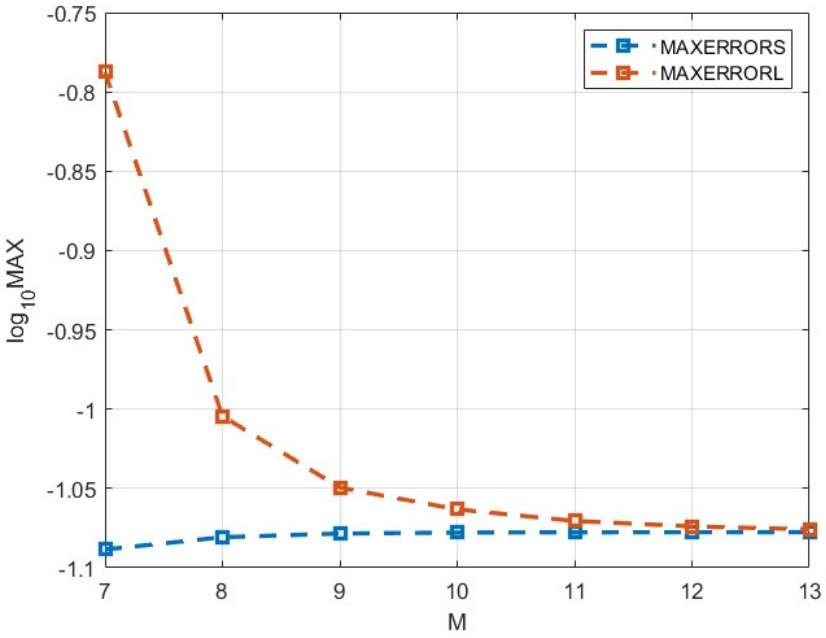

Figure 19: Max Error in log-scale, varying M, for spline and linear interpolation

5 Pricing of a Sprint Autocallable Put Option

Using the simulation of the underlying price S_{t_i} with ATS increments on monitoring dates $t_0, ..., t_Q$, we have attempted to price a Sprint Autocallable Put option with K=2500. This exotic derivative pays (once and then the product is called) at 12 dates t_i from t_1=9-Jul-2019 to t_{12}=9-Jun-2020:

$$\frac{1}{S_0} max\left(K - S_{t_i}, 0\right) \cdot \frac{1}{S_0} \max_{j<i} S_{t_j}$$

Where the monitoring dates are two business days before the payment ones, according to modified following business day convention. Moreover if the above condition is never satisfied, the derivative has null payoff at the expiry.
In order to price this contract we needed the ATS parameters at the monitoring dates for the Lewis FFTS simulations. To find them we have interpolated the ones obtained from the calibration in 4.2. using different techniques according to the parameters. From the graph below it is possible to see that interpolation for k and σ is almost equivalent using linear or spline, while for the third parameter η in some cases the difference between the two approaches is not negligible. For this reason we have decided to proceed with the pricing taking into account the linear interpolation for k and σ and the spline procedure for η.

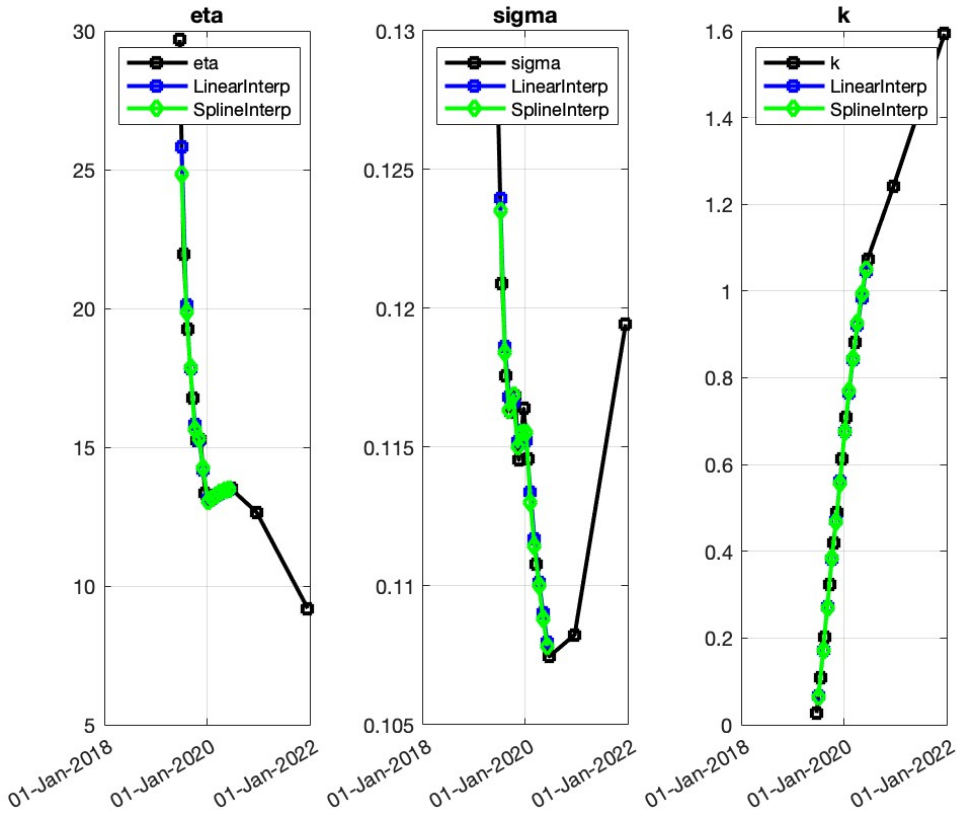

Figure 20: η_t, σ_t, k_t interpolated parameters

After having obtained the parameters at the needed dates, the simulation of the ATS increments $f_t - f_s$ (with t and s monitoring dates) has been performed, in order to simulate the paths of the underlying at each monitoring date the procedure described in 4.4.5 has been used.

$$S_t = F(s,t)e^{f_t - f_s}$$

We have got the price of this exotic option as the sum of discounted means of the simulated payoffs, paying attention to when the underlying went under the strike, since in these cases, by definition of the contract, the first time the option is in the money it is called and it ends. For this reason we have considered a non-null payoff only when the strike was lower than the minimum value of the underlying till that date.

To verify the price obtained, we have performed another pricing procedure using an Exponential Lévy Monte Carlo simulation and considering in this case the constant optimal NIG parameters σ,η, κ derived from the LTS NIG calibration. In order to proceed in this way we have simulated as in 2.1. the LTS process:

$$f_t = -\left(\frac{1}{2} + \eta\right)\Delta t\sigma^2 G + \sigma\sqrt{\Delta t}\sqrt{G}g - \ln \mathcal{L}(\eta)$$

where g is a simulated Standard Normal random variable, G is a simulated Inverse Gaussian random variable with unitary mean and variance $k/\Delta t$, and $-\ln \mathcal{L}(\eta)$ is the log-Laplace transform deriving from the martingale condition on the forward. For the evaluation of the payoff we have proceeded as before evaluating the conditions at monitoring dates.
As last check we have priced the option using again the Lewis FFTS simulations for the underlying price, but taking into account the parameters in the table in 4.3. coming from the fitting of a power-law ATS. We have confronted the results toghether with the corresponding confidence intervals in the table below:

Model	Price	CI 95 %
ATS NIG	0.0234 €	[0.0232, 0.0235] €
LTS NIG	0.0234 €	[0.0232, 0.0235] €
PL ATS NIG	0.0232 €	[0.0230, 0.0233] €

As we can see, the prices obtained with different procedures are consistent and so we have decided to consider the contract correctly evaluated.

6 Conclusion

In this work we have investigated the properties of Additive Tempered Stable (ATS) processes that, thanks to time-inhomogeneity, allowed us to overcome the limits of Lévy Normal Tempered Stable (LTS) processes. We have calibrated the ATS processes using the most liquid options of S&P 500 index, highlighting the enhancements with respect to the LTS calibration procedure. It immediately jumps to the eye how relevant is the improvement of ATS NIG especially for short maturities where classical LTS NIG is very inaccurate.

We have observed that ATS processes have excellent calibration features on the equity volatility surface and present interesting scaling properties. Indeed from calibrated parameters, we have been able, via linear regressions, to estimate the parameters of a Power-Law ATS process. Another important fact is that these processes allow for time changes.

Moreover, this class of models have revealed to be really efficient also for pricing purposes enjoying a simple Monte Carlo scheme faster than the one of normal LTS. Indeed this takes advantage of both the efficiency of the FFT algorithm, applied to the Lewis formula in order to obtain the CDF of process increments, and the spline interpolation properties when inverting it.

As last application we have employed the former simulation for pricing purposes, both for European call options and for an exotic path-dependent product. For plain vanilla options the results are almost the same of the ones obtained via Lewis closed formula and the price of a Sprint Autocallable Put Option is coherent with the one simulating the underlying as NIG (time-homogeneous) model.

Combining an accurate reproduction of volatility surface making use of few parameters, with good applicability to fast and precise pricing techniques, ATS processes can be considered a very interesting modeling choice in quantitative finance.

A Appendix

We have reported in this appendix the results of the calibration on ITM options, which we have discarded for a reason of liquidity. The procedure followed is exactly the same of the one described in 4.2.. As before we report the smiles obtained for the same three different maturities:

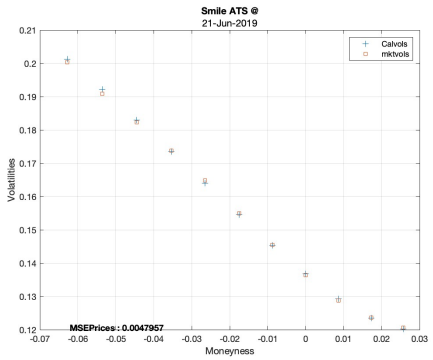

Figure 21: First maturity smile ITM

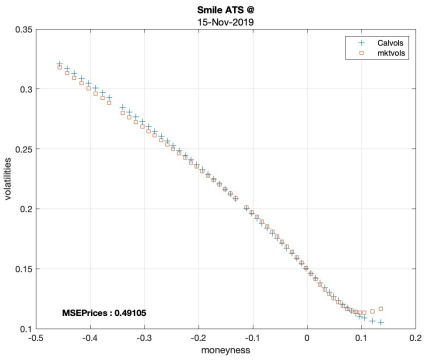

Figure 22: Intermediate maturity smile ITM

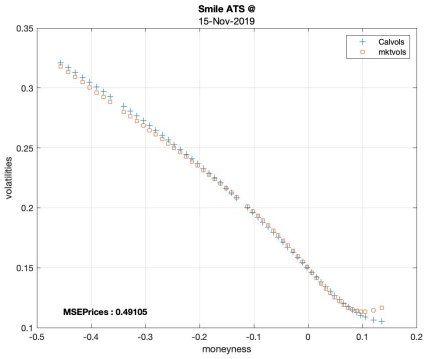

Figure 23: Last maturity smile ITM

Below it is presented also a small summary of the performances of this calibration. Comparing with table 3, it is possible to notice that these results are slightly better. However we have decided to discard this calibration driven by the fact that in financial markets, the most reliable prices are the ones of the most liquid options.

Maturity	ATS MAPE	ATS MSE
21-Jun-2019	0.0912 %	0.0048
15-Nov-2019	0.2110 %	0.4910
17-Dec-2021	0.1796 %	1.909

Table 7: Calibration performances ITM options

References

[1] Azzone, M., and R. Baviera. *A fast Monte Carlo scheme for additive processes and option pricing*. arXiv preprint arXiv:2112.08291 (2021).

[2] Azzone, M. and R. Baviera. *Additive normal tempered stable processes for equity derivatives and power-law scaling*. Quantitative Finance 22.3 (2022): 501-518.

[3] Azzone, M., and R. Baviera. *Synthetic forwards and cost of funding in the equity derivative market*. Finance Research Letters 41 (2021): 101841.

[4] Carr, P. and Madan, D., *Option valuation using the fast Fourier transform. J.* Comput. Finance, 1999, 2(4), 61–73

[5] Glasserman, P. and Liu, Z., 2010. *Sensitivity estimates from characteristic functions* Operations Research, 58 (6), 1611–1623.